

Mode optimization for quantum-state tomography with array detectors

A. M. Dawes and M. Beck*

Department of Physics, Whitman College, Walla Walla, Washington 99362

K. Banaszek

University of Oxford, Clarendon Laboratory, Parks Road, Oxford, OX1 3PU, United Kingdom

(Received 31 October 2002; published 11 March 2003)

We demonstrate that it is possible to choose an optimal signal mode for state reconstruction when performing quantum-state tomography with array detectors. The mode optimization is done during the data analysis (i.e., after all the data have been collected.) We develop theoretically a procedure for finding the mode that satisfies a criterion which is quadratic in field operators; as examples we explicitly show how to maximize the average photon number, or the amount of quadrature squeezing. We experimentally demonstrate the technique by finding the mode which maximizes the average photon number for coherent-state signal beams occupying both linear and sinusoidal modes.

DOI: 10.1103/PhysRevA.67.032102

PACS number(s): 03.65.Wj, 03.65.Ta, 42.50.Ar

I. INTRODUCTION

Quantum-state tomography (QST) describes the process of performing a large ensemble of measurements on a quantum system, and then analyzing the measured data in such a way as to determine the full-quantum-mechanical state of the system. The ideas behind QST are sufficiently general that they apply, in somewhat different forms, to different types of optical systems [1–7], molecular vibrations [8], trapped ions [9], and atomic beams [10]. Extensions of QST have been made to include multiple-mode systems [11–15]. Recently it has been shown that the use of array detectors can significantly improve the optical version of QST [16–18].

To date experiments have demonstrated two types of improvements afforded by array detectors. The first is that array detectors can increase the effective detection efficiency over standard detectors when using balanced homodyne detection. This increase is due to the fact that the local oscillator (LO) and signal fields need not be mode-matched when using array detectors. In Ref. [17] array detection was found to be over 40 times more efficient than standard detection for measurements of a particular field mode. The second improvement is that arrays allow the experimenter to simultaneously determine the state of many different field modes. This comes about because the measured mode is not determined during the data acquisition, but is instead chosen during the numerical postprocessing. Thus, one can choose to determine the state of any mode during the analysis (subject to the constraint that the mode function must be real) [16,17].

In a practical situation, the shape of the signal mode that exhibits some property of interest, such as quadrature squeezing, is not known exactly before the measurement. In a standard homodyne setup with point detectors the mode containing the desired feature of the output is selected by careful control of the spatiotemporal shape of the LO field; the measured signal mode is essentially the projection of the signal onto the LO mode. Creating an LO in an arbitrary

mode is an extremely difficult task experimentally, and it becomes even more difficult if the experimenter is not completely sure about what mode shape needs to be created.

Because array detection affords the opportunity to measure essentially any mode, a question that naturally arises is: can one choose this mode in an intelligent fashion? That is, can one somehow find a particular mode in a signal field that has some desired property? For example, could one determine which mode contains the largest average photon number, or the largest amount of quadrature squeezing? Then, once the corresponding mode function is known its quantum state could easily be determined. Throughout this paper, we will refer to the mode whose state best fits some criteria as the “optimal” mode. We will further refer to the process of finding this mode as mode optimization.

It is certainly possible to imagine performing mode optimization using data acquired with an array detector. If by no other means, one could use a brute-force optimization technique: choose a mode function, determine the state of that mode, see how well that state fits your definition of optimal, choose another mode function and repeat. There is certainly no guarantee that such a brute-force approach would yield the globally optimal solution, and it would be a tedious process; however, after doing this you would almost certainly end up with a solution that was better than if you had just taken your best guess as to what the optimal mode function should be.

Here, we demonstrate that it is not necessary to resort to such a crude, brute-force optimization technique, at least when the quantity of interest is quadratic in the quadrature amplitude operators. Specifically, we shall consider two criteria: maximization of the average photon number, and minimization of the quadrature variance. We will describe the theory behind the optimization process, and provide the results of experiments that maximize the average detected photon number for signal fields in weak coherent states.

II. THEORY

For simplicity we will discuss here the one-dimensional case, which is the case in our experiments. Generalization to

*FAX: 509-527-5904; Email address: becmk@whitman.edu

two-dimensional mode functions is straightforward. Let us assume that the mode of interest is described by a real valued spatial function $u_m(x)$. *A priori* the form of this function is not known, and it should be derived from the optimization criterion. Following Ref. [16], the quadrature amplitude operator for this mode is given by

$$\hat{q}_{m\phi} = \frac{1}{\beta} \left(\frac{D_x}{2} \right)^{1/2} \sum_j \Delta \hat{N}_{j\phi} u_m(x_j), \quad (1)$$

where ϕ and β are, respectively, the phase and the amplitude of the LO used for homodyning; the LO is assumed to be in a plane-wave mode. In Eq. (1), D_x is the spatial extent of the detector array, and $\Delta \hat{N}_{j\phi}$ is the operator of the difference photocounts measured at the j th pixel for the local oscillator phase ϕ .

As the first optimization criterion, we shall consider maximization of the average number of photons. The photon number operator \hat{n}_m for the mode m is given by the standard formula

$$\hat{n}_m = \frac{1}{2\pi} \int_0^{2\pi} d\phi \hat{q}_{m\phi}^2 - \frac{1}{2}. \quad (2)$$

Using Eq. (1), we can express this operator in terms of the difference photocounts $\Delta \hat{N}_{j\phi}$ as

$$\hat{n}_m = \frac{D_x}{4\pi\beta^2} \sum_{jj'} \int_0^{2\pi} d\phi \Delta \hat{N}_{j\phi} \Delta \hat{N}_{j'\phi} u_m(x_j) u_m(x_{j'}) - \frac{1}{2}. \quad (3)$$

Evaluating the expectation value of both sides of this expression yields

$$\langle \hat{n}_m \rangle = \frac{D_x}{2\beta^2} \mathbf{u}^T \cdot \mathbf{M} \cdot \mathbf{u} - \frac{1}{2}, \quad (4)$$

where we have introduced vector notation. In this notation \mathbf{M} is the correlation matrix for the difference photocounts, averaged over the phase of the local oscillator:

$$\mathbf{M}_{jj'} = \frac{1}{2\pi} \int_0^{2\pi} d\phi \langle \Delta \hat{N}_{j\phi} \Delta \hat{N}_{j'\phi} \rangle \quad (5)$$

and $\mathbf{u} = u_m(x_j)$ is a vector composed from the values of the mode function taken at the pixels of the array detector. Normalization of the mode function implies a constraint on the length of the vector \mathbf{u} in the form

$$\mathbf{u}^T \cdot \mathbf{u} = \sum_j u_m^2(x_j) = \frac{1}{\delta x}, \quad (6)$$

where δx is the width of an individual pixel [16].

As the second term on the right-hand side of Eq. (4) is constant, the problem of selecting the optimal mode reduces to maximizing the quadratic form defined by the correlation matrix \mathbf{M} . This task is in turn equivalent to finding the eigenvector of \mathbf{M} corresponding to its maximum eigenvalue, which can be seen from the following reasoning. Let us de-

note by μ_k the eigenvalues of \mathbf{M} , arranged in descending order, and by \mathbf{v}_k the corresponding eigenvectors, assumed to be normalized according to Eq. (6). As the correlation matrix \mathbf{M} is real and symmetric, these eigenvectors are mutually orthogonal. Any vector \mathbf{u} satisfying Eq. (6) can be represented as a linear combination $\mathbf{u} = \sum_k c_k \mathbf{v}_k$ of the eigenvectors with certain real coefficients c_k whose squares sum to $\sum_k c_k^2 = 1$. Then the value of the quadratic form has the upper bound given by

$$\mathbf{u}^T \cdot \mathbf{M} \cdot \mathbf{u} = \sum_k \mu_k c_k^2 \mathbf{v}_k^T \cdot \mathbf{v}_k \leq \mu_1 \sum_k c_k^2 \frac{1}{\delta x} = \frac{1}{\delta x} \mu_1. \quad (7)$$

The above inequality becomes an equality if the vector \mathbf{u} is an eigenvector of \mathbf{M} corresponding to its largest eigenvalue.

This eigenvector \mathbf{u} corresponding to the largest eigenvalue defines the shape of the optimal mode $u_{\text{opt}}(x_j)$. Since the correlation matrix \mathbf{M} is real and symmetric, the eigenvalue problem can be solved using one of the standard numerical algorithms for this class of matrices [19]. If the number of pixels is excessively large, one can alternatively use methods designed specifically to find only the extreme eigenvalues [20]. In principle, the maximum eigenvalue of the correlation matrix can be degenerate, corresponding to more than one eigenvector. In practice, however, if the spatial structure of signal field is not overly complicated the matrix \mathbf{M} can be reasonably expected to possess a nondegenerate largest eigenvalue clearly separated from all the other eigenvalues.

Once the optimal mode has been determined as described above, it can then be substituted for $u_m(x_j)$ in Eq. (1), and the quadrature amplitudes corresponding to this mode can be computed. These amplitudes can then be used to determine the quantum state of the field using any of a number of different algorithms (see Refs. [3], [4] for some examples). In our case, we determine the density matrix of the mode in the Fock state basis.

An analogous discussion can be carried out when the quantity of interest is squeezing of the quadrature noise variance $\Delta q_{m\phi}^2$. In this case, a calculation analogous to the previous one shows that the variance of the quadrature amplitude $q_{m\phi}$ detected for the LO phase ϕ can be written in vector form as

$$\Delta q_{m\phi}^2 = \langle \hat{q}_{m\phi}^2 \rangle - \langle \hat{q}_{m\phi} \rangle^2 = \frac{D_x}{2\beta^2} \mathbf{u}^T \cdot \mathbf{S}_\phi \cdot \mathbf{u}, \quad (8)$$

where \mathbf{S}_ϕ is the covariance matrix of difference photocounts for the local oscillator phase ϕ , defined as

$$\mathbf{S}_\phi = \langle \Delta \hat{N}_{j\phi} \Delta \hat{N}_{j'\phi} \rangle - \langle \Delta \hat{N}_{j\phi} \rangle \langle \Delta \hat{N}_{j'\phi} \rangle. \quad (9)$$

The optimization problem is similar to the previous one, except that now we need to find the eigenvector corresponding to the minimum eigenvalue of the matrix \mathbf{S}_ϕ . In addition, the eigenvalue problem has to be solved separately for each of the phases ϕ used in the experiment in order to find the setting of the LO phase that yields the strongest squeezing.

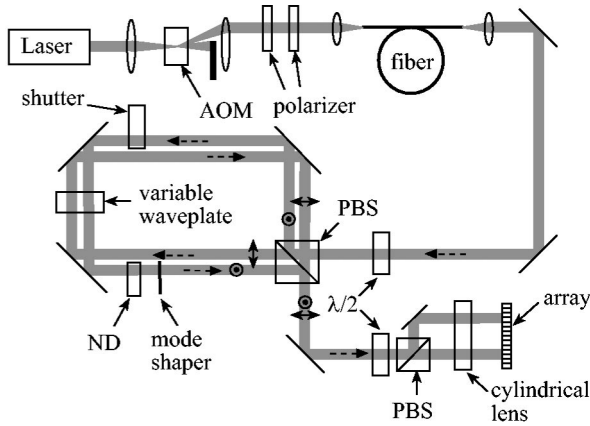


FIG. 1. The experimental apparatus: ND stands for neutral-density filter, PBS stands for polarizing beam splitter, and AOM stands for acousto-optic modulator. In the near common-path interferometer the polarizations and directions of the beams are indicated. The AOM, shutter, variable wave plate and CCD array are all under computer control.

We note that we are able to resort to standard numerical methods for solving symmetric eigenvalue problems because the quantity used as the optimization criterion is quadratic in the quadrature amplitude operators. In a general case the optimization criterion can be a highly nonlinear function, which makes the optimization problem significantly more complicated.

III. EXPERIMENTAL SETUP

The experimental arrangement is nearly the same as that used in Ref. [17], and a schematic is shown in Fig. 1. We use a frequency doubled Nd:YVO₄ laser, which produces a continuous-wave output at 532 nm, as our light source. An acousto-optic modulator acts as a shutter to produce 10-ms-long light pulses synchronized with the exposure time of the charge-coupled device (CCD) array. A polarizer-analyzer pair adjusts the light intensity, and a single-mode optical fiber spatially filters the beam.

A $\lambda/2$ plate allows us to adjust the splitting ratio on a polarizing beam splitter (PBS) that constitutes the entrance to a near common-path interferometer. The signal beam exits the beam splitter vertically polarized and travels counter-clockwise around the ring, while the LO is horizontally polarized and travels clockwise. The relative phase of the two beams is adjusted with a liquid crystal variable wave plate whose axes are aligned so that it provides a $0-2\pi$ rad phase shift to the LO, but does not affect the signal beam.

We modify the spatial structure of the signal beam with a mode shaper, as discussed further below. The signal and the LO return to the PBS and emerge from the interferometer spatially overlapped, but with orthogonal polarizations. After leaving the interferometer the beams pass through another combination of a $\lambda/2$ plate and a PBS. The $\lambda/2$ plate rotates the polarizations of the signal and the LO beams, so that they are at 45° with respect to the axes of the PBS, so the PBS acts as a 50:50 beam splitter on which the signal and local oscillator beams interfere. The beams emerging from the

PBS are focused perpendicular to the plane of Fig. 1 with a cylindrical lens, and are detected on spatially separate regions of a CCD array.

The CCD is a 100×1340 array of $20 \times 20 \mu\text{m}^2$ pixels. It has a quantum efficiency of $\approx 90\%$ at 532 nm and is cooled to -110°C yielding a negligible dark-count rate of less than 1 electron per pixel per hour. The read out rate for each exposure is ≈ 15 Hz.

Registering the pixels on the two outputs to ensure proper subtraction is extremely important in these experiments. If the pixels are not properly registered, we are unable to achieve shot-noise limited detection. Pixel registration is accomplished with the signal beam blocked, so that the signal is in a vacuum state. The procedure is a combination of finely adjusting the optical alignment and numerically adjusting the center pixels of the two images.

Finally, in order to eliminate offsets in our quadrature measurements, we measure the average vacuum difference level by blocking the signal beam after measurement of each LO phase. This vacuum level is subtracted from the measured difference number to yield the corrected difference number $\Delta N_j - \langle \Delta N_j \rangle_{\text{vac}}$. We actually use the corrected difference number in place of ΔN_j in Eq. (1) when we calculate the quadrature amplitudes. Further details of how we detect the beams, register the pixels on the two outputs, determine the LO amplitude β , and subtract the vacuum signal level can be found in Ref. [17].

IV. EXPERIMENTAL RESULTS

The first signal mode we examined was one whose electric field varied linearly across the surface of the detector. Mathematically, the field mode we were attempting to duplicate was one whose functional form was

$$u_{\text{lin}}(x) = \left(\frac{12}{D_x^3} \right)^{1/2} x. \quad (10)$$

Experimentally, we do this by inserting a microscope cover slip halfway into the signal beam. The tilt angle of the cover slip is adjusted to provide a π (or an odd multiple of π) phase shift between the two halves of the beam. Near its center, the far-field diffraction pattern of a beam modified in this way is that of a linear electric field.

In Fig. 2(a), we show the corrected difference number as a function of pixel number across the array. This is for a single exposure of the array, and thus contains all of the quantum noise associated with detecting a very weak signal beam. We collect 36 200 shots of such data (200 shots/phase angle, 181 phase angles varying between 0 and 2π), compute the correlation matrix [Eq. (5)], diagonalize the matrix and determine the eigenmode corresponding to the largest eigenvalue. This is the mode $u_{\text{opt}}(x)$ that maximizes the average photon number, and it is also plotted in Fig. 2(a). This mode is found to have an average photon number of 2.3, and has a nearly linear variation with position, as expected.

Now that we have determined the optimal mode function $u_{\text{opt}}(x)$, we substitute it for the measured mode function $u_m(x)$ in Eq. (1) to determine the quadrature amplitudes of

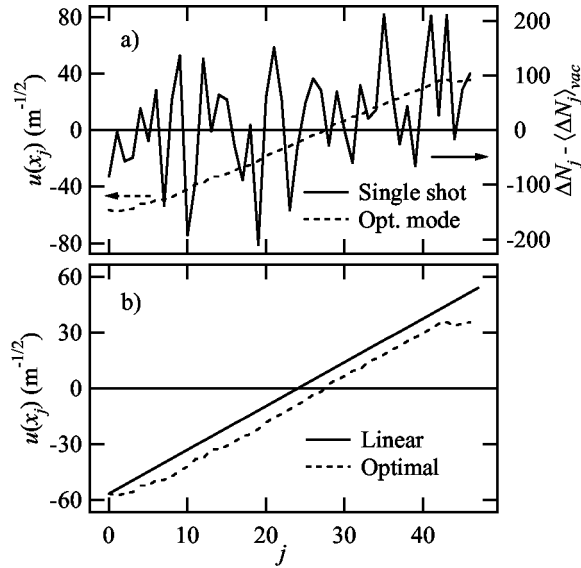


FIG. 2. In (a), we show the corrected difference number as a function of pixel number against the right axis for a signal mode that varies linearly across the detector. Plotted against the left axis is the mode that maximizes the average photon number. In (b), we compare the optimal mode to an *a priori* “best guess” linear mode.

our individual exposures. These quadrature amplitudes are then used to find the quantum state of this mode using QST. We determine the state in terms of its density-matrix representation in the Fock state basis. In Fig. 3, we plot the experimentally determined photon number distribution $P(n)$ for this optimal mode. Also shown in Fig. 3 is the distribution for a theoretical coherent state with the same average photon number. We see that our state is reasonably well described by a coherent state.

In Fig. 2(b), we show a comparison between the optimal mode and a purely linear mode [Eq. (10)]. This linear mode represents an *a priori* “best guess” as to what mode we would expect to see in this experiment. We can calculate the state of this linear mode, and also determine its average photon number, and we find that it has an average of 2.2 photons. This means that our optimal mode has a slightly higher average photon number, but our best guess was still reason-

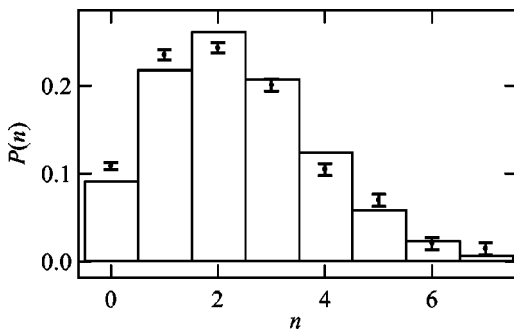


FIG. 3. Photon number distribution of the measured state corresponding to the optimal mode when the signal varies linearly across the array. The points represent measured values, while the bars correspond to a theoretical coherent state having the same mean number of photons. The average photon number is 2.3.

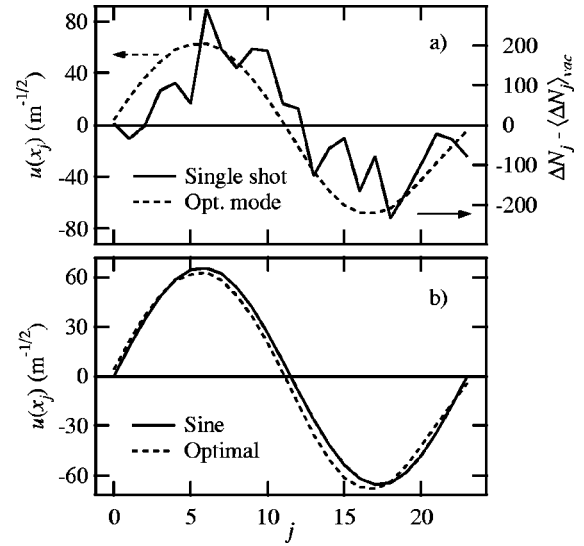


FIG. 4. In (a), we show the corrected difference number as a function of pixel number against the right axis for a signal mode that varies sinusoidally across the detector. Plotted against the left axis is the mode that maximizes the average photon number. In (b), we compare the optimal mode to an *a posteriori* sinusoidal mode having the same period and phase as the optimal mode.

ably good in this case. Finally, we can compute what we would have got if we had used point detectors instead of array detectors. We do this by finding the state corresponding to a mode that is constant across the face of the detector. We find this mode to have an average of 0.4 photons, so we get about a five-fold increase in detection efficiency when using array detectors to detect this particular signal mode with a plane-wave LO.

We have also examined a signal mode that has a sinusoidal variation of electric field across the array. We create this field by using a double slit as our mode shaper, which produces a sinusoidal field in the far field. Figure 4(a) shows the corrected difference number taken from a single exposure of the array, as well as the optimal mode computed from 36 200 exposures. The single exposure data here looks less noisy than in Fig. 2(a), but the main reason for this is that the signal level is higher in this case. We find the optimal mode here to have an average of 4.8 photons.

Before computing the state of this signal mode, we make one more correction to our data that we did not need to make to the linear mode data. Because the slits block a large fraction of the signal beam in the interferometer, we must have substantially more light present in the signal arm of the interferometer. We find that this light creates a background on our array that must be accounted for. Subtraction of the vacuum signal as described above eliminates imbalance in the LO, but since the signal is blocked in order to do this correction it cannot eliminate background associated with the signal beam. We eliminate this background on the signal by noting that because $\hat{q}_{m\phi+\pi} = -\hat{q}_{m\phi}$ the phase average of the quadrature amplitudes must be zero:

$$\int_0^{2\pi} d\phi \langle \hat{q}_{m\phi} \rangle = 0. \quad (11)$$

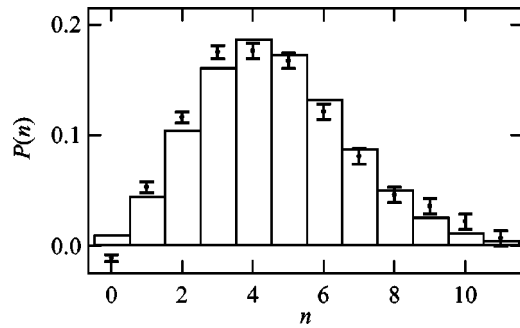


FIG. 5. Photon number distribution of the measured state corresponding to the optimal mode when the signal varies sinusoidally across the array. The points represent measured values, while the bars correspond to a theoretical coherent state having the same mean number of photons. The average photon number is 4.8.

Any difference from zero is attributable to background in our signal beam, so we subtract off this difference from the quadrature amplitudes before computing the quantum state.

The photon number distribution for this mode is shown in Fig. 5, and once again we find that our state is reasonably well described by a coherent state. It is interesting to note that Fig. 5 indicates there is a very small probability that this state contains more than 10 photons. Using the generous assumption of 10 photons and looking back at Fig. 4(a) shows that on this single shot there is less than 1/2 a signal photon per pixel (there are thousands of LO photons per pixel), yet we still see a strong interference pattern. So, thinking in terms of photons makes the single-shot data of Fig. 4(a) seem surprising indeed.

In Fig. 4(b), we show a comparison between the optimal mode and a pure sinusoidal mode. In this case, the sinusoidal mode was not chosen using *a priori* knowledge of the mode, but was instead chosen *a posteriori* given the optimal mode; it is the sinusoidal mode that has the same period and phase as the optimal mode. This mode is found to have a mean of 4.6 photons. This is fairly close to the optimal value, and this is not surprising because the modes are seen to be nearly the same in Fig. 4(b).

By looking solely at the measured difference numbers in Fig. 4(a), one might at first glance think that the optimal mode would have a slightly smaller period than the one found from the algorithm. However, by using a sinusoidal mode that, by eye, appears to fit this corrected difference data better, we obtain a measured average photon number of only 3.6 photons. In this case, the algorithm works significantly better than the eye. We also find that single area-integrating detectors would measure a state with an average of only 0.13 photons, so once again we find that arrays offer a dramatic improvement over single detectors.

V. CONCLUSIONS

We have shown that it is possible to find the “optimal” signal mode when performing quantum-state tomography with array detectors. Here, we have explicitly derived the procedures necessary to find the mode which maximizes the average photon number, or maximizes the amount of quadra-

ture squeezing. We have experimentally demonstrated the technique for maximizing the average photon number.

In addition to the obvious benefits, mode optimization offers other important information to the experimenter as well. For instance, in the experiments with a double slit in our signal beam we expected to see sinusoidal fringes emerge as being the optimal mode. In runs where this was not the case, it indicated to us that there was likely an alignment error somewhere in our system. Thus, finding the optimal mode provided information that helped us to improve the alignment of our system; something that *a priori* knowledge of what the mode should look like could never do by itself.

In some cases finding the optimum mode might be even more interesting than finding the quantum state. For example, consider the case of the squeezed mode generated in a traveling wave optical parametric amplifier pumped with a Gaussian beam. Of course, one wishes to find the maximal squeezing, but it is especially interesting to examine what the exact shape of this maximally squeezed mode is. There are a few references that discuss theoretically this problem [21–23]. There have also been experiments that generate an LO mode that better matches this squeezed mode, and hence observe larger amounts of squeezing [24]. However, there has been no experimental effort to date on explicitly searching out the mode that truly maximizes the amount of squeezing. Such experiments are possible using array detectors.

Experiments detecting nonclassical light with arrays would be difficult, but we believe that they should not be any more difficult than similar experiments with point detectors. One big challenge is in registering pixels on the two images. As described above, registration is done with a vacuum signal beam (the average difference numbers and the noise level of the difference numbers are quite sensitive to pixel registration) so registration should be no more difficult with nonclassical signal beams than it is with classical beams. Also, the phase fronts and timing of the signal and the LO beams must be matched, but this is also the case in experiments involving point detectors, and experimenters have developed ingenious schemes for doing this (see, for example, Ref. [25].) Indeed, this alignment may be easier to do with array detectors because the experimenter will likely have *some* idea of what the optimal mode shape will be (e.g., it will likely be shaped like a “bump” as opposed to having fringes across it), and this can be used to improve the alignment of the phase fronts.

Ideally one would like to have a means of using unbalanced array detection in order to eliminate the need to register pixels. Unbalanced array detection has been used in measurements of the Q function [18], but so far has not been demonstrated for Wigner function or density-matrix measurements. We are currently exploring possibilities for unbalanced measurements of the density matrix.

ACKNOWLEDGMENTS

This work was supported by the National Science Foundation and by Whitman College. K.B. would like to acknowledge support from ARDA Grant No. P-43513-PH-QCO-02107-1.

- [1] K. Vogel and H. Risken, *Phys. Rev. A* **40**, 2847 (1989).
- [2] D. T. Smithey, M. Beck, M. G. Raymer, and A. Faridani, *Phys. Rev. Lett.* **70**, 1244 (1993); D. T. Smithey, M. Beck, J. Cooper, M. G. Raymer, and A. Faridani, *Phys. Scr.*, T **T48**, 1514 (1993).
- [3] U. Leonhardt, *Measuring the Quantum State of Light* (Cambridge University Press, Cambridge, England, 1997).
- [4] G. M. D'Ariano, in *Quantum Optics and the Spectroscopy of Solids*, edited by T. Hakioglu and A. S. Shumovsky (Kluwer, Dordrecht, 1997), p. 139.
- [5] D. G. Welsch, W. Vogel, and T. Opatrny, in *Progress in Optics* (North-Holland, Amsterdam, 1999) Vol. XXXIX, p. 63.
- [6] A. G. White, D. F. V. James, P. H. Eberhard, and P. G. Kwiat, *Phys. Rev. Lett.* **83**, 3103 (1999).
- [7] K. Banaszek, C. Radzewicz, K. Wodkiewicz, and J. S. Krasinski, *Phys. Rev. A* **60**, 674 (1999).
- [8] T. J. Dunn, I. A. Walmsley, and S. Mukamel, *Phys. Rev. Lett.* **74**, 884 (1995).
- [9] D. Leibfried, D. M. Meekhof, B. E. King, C. Monroe, W. M. Itano, and D. J. Wineland, *Phys. Rev. Lett.* **77**, 4281 (1996).
- [10] S. Schiller, G. Breitenbach, S. F. Pereirs, T. Muller, and J. Mlynek, *Phys. Rev. Lett.* **77**, 2933 (1996).
- [11] H. Kuhn, D.-G. Welsch, and W. Vogel, *Phys. Rev. A* **51**, 4240 (1995).
- [12] M. G. Raymer, D. F. McAlister, and U. Leonhardt, *Phys. Rev. A* **54**, 2397 (1996).
- [13] G. M. D'Ariano, M. F. Sacchi, and P. Kumar, *Phys. Rev. A* **61**, 013806 (1999).
- [14] M. G. Raymer and A. C. Funk, *Phys. Rev. A* **61**, 015801 (1999).
- [15] M. Vasilyev, S.-K. Choi, P. Kumar, and G. M. D'Ariano, *Phys. Rev. Lett.* **84**, 2354 (2000).
- [16] M. Beck, *Phys. Rev. Lett.* **84**, 5748 (2000).
- [17] A. M. Dawes and M. Beck, *Phys. Rev. A* **63**, 040101(R) (2001).
- [18] M. Beck, C. Dorrer, and I. A. Walmsley, *Phys. Rev. Lett.* **87**, 253601 (2001).
- [19] W. H. Press, S. A. Teukolsky, W. T. Vetterling, and B. P. Flannery, *Numerical Recipes* (Cambridge University Press, Cambridge, 1992), Chap. 11.
- [20] B. N. Parlett, *The Symmetric Eigenvalue Problem* (Prentice-Hall, Englewood Cliffs, NJ, 1980).
- [21] A. La Porta and R. E. Slusher, *Phys. Rev. A* **44**, 2013 (1991).
- [22] R.-D. Li and P. Kumar, *J. Opt. Soc. Am. B* **12**, 2310 (1995).
- [23] J. H. Shapiro and A. Shakeel, *J. Opt. Soc. Am. B* **14**, 232 (1997).
- [24] C. Kim and P. Kumar, *Phys. Rev. Lett.* **73**, 1605 (1994).
- [25] A. I. Lvovsky, H. Hansen, T. Aichele, O. Benson, J. Mlynek, and S. Schiller, *Phys. Rev. Lett.* **87**, 050402 (2001).